

Code equations

Yvonne Ban

3 June 2019

Contents

| | | |
|----------|---|-----------|
| 1 | Empirical inputs | 4 |
| 2 | Constants | 4 |
| 2.1 | VI, volume of inductor | 4 |
| 2.2 | nsq, number of squares of inductor | 5 |
| 2.3 | nu_opt, frequency of photons | 5 |
| 2.4 | E_gamma, energy of photons | 5 |
| 2.5 | delta0, gap energy at 0K | 5 |
| 2.6 | delta, gap energy at T | 6 |
| 2.7 | sigma_n, normal conductivity just above Tc | 6 |
| 2.8 | lambL, (London) penetration depth in the thin film limit | 6 |
| 2.9 | N0, single-spin density of electron states at Fermi energy | 7 |
| 2.10 | N_qp_photon, number of quasiparticles produced per photon | 7 |
| 3 | Intrinsic parameters (intrinsic to material) | 7 |
| 3.1 | R_qp, intrinsic quasiparticle recombination constant | 7 |
| 4 | Thermal parameters (depend on T) | 8 |
| 4.1 | n_qp_therm, quasiparticle density due to thermal effects at T | 8 |
| 4.2 | gamma_G, low-temperature thermal generation rate at T | 8 |
| 5 | Steady-state parameters | 8 |
| 5.1 | tau_phon_es, phonon escape time | 8 |
| 5.2 | F_phon, phonon trapping factor | 9 |
| 5.3 | R_eff, effective quasiparticle recombination constant | 9 |
| 5.4 | tau_qp, quasiparticle relaxation time | 10 |
| 5.5 | n_qp_ss, steady-state quasiparticle density | 10 |
| 5.6 | N_qp_ss, steady-state quasiparticle number in resonator | 10 |
| 6 | Optical generation | 11 |
| 6.1 | gamma_opt, constant optical power quasiparticle generation rate | 11 |

| | | |
|-----------|---|-----------|
| 7 | All together now | 11 |
| 7.1 | N_{qp_tot} , total number of quasiparticles in resonator due to thermal and constant optical power effects | 11 |
| 8 | Complex conductivity | 12 |
| 8.1 | σ_{1_0} , real part of complex conductivity at $T=0K$ | 12 |
| 8.2 | σ_{2_0} , imag part of complex conductivity at $T=0K$ | 12 |
| 8.3 | σ_{1rat} , ratio of real part of complex conductivity to quasiparticle density response at T | 12 |
| 8.4 | σ_{2rat} , ratio of imag part of complex conductivity to quasiparticle density response at T | 13 |
| 8.5 | σ_1 , real part of complex conductivity at T | 13 |
| 8.6 | σ_2 , imag part of complex conductivity at T | 13 |
| 8.7 | σ , complex conductivity at T | 14 |
| 9 | Surface impedance, reactance, (kinetic) inductance, resistance | 14 |
| 9.1 | Z_{s_0} , surface impedance in thin film local limit at $T=0K$ | 14 |
| 9.2 | Z_s , surface impedance in thin film local limit at T | 15 |
| 9.3 | X_{s_0} , surface reactance in thin film local limit at $T=0K$ | 15 |
| 9.4 | X_s , surface reactance in thin film local limit at T | 15 |
| 9.5 | R_s , surface resistance in thin film local limit at T | 16 |
| 9.6 | L_{k_0} , kinetic inductance in thin film local limit at $T=0K$ | 16 |
| 9.7 | L_k , kinetic inductance in thin film local limit at T | 16 |
| 10 | Resonant frequency | 17 |
| 10.1 | α , effective kinetic inductance fraction in thin film local limit | 17 |
| 10.2 | f_0 , resonant frequency of resonator circuit at $T=0K$ | 17 |
| 10.3 | f_{frac} , fractional frequency shift in resonant frequency of circuit | 18 |
| 10.4 | f_{new} , resonant frequency of resonator circuit in thin film local limit | 18 |
| 10.5 | f_{det} , detuning of resonant frequency from readout frequency | 18 |
| 11 | Quality factors | 19 |
| 11.1 | Q_{qp} , quality factor of resonator circuit from quasiparticles | 19 |
| 11.2 | Q_r , quality factor of resonator circuit in thin film local limit | 19 |
| 12 | Responsivities | 20 |
| 12.1 | dP_{abs}/dP_{inc} , responsivity of absorbed optical power to incident optical power | 20 |
| 12.2 | $d\Gamma/dP$, responsivity of quasiparticle generation rate to optical power . | 20 |
| 12.3 | $dN_{qp_tot}/d\Gamma$, responsivity of N_{qp_tot} to quasiparticle generation rate | 20 |
| 12.4 | $d\sigma_1/dN$, responsivity of σ_1 to N_{qp_tot} | 21 |
| 12.5 | $d\sigma_2/dN$, responsivity of σ_2 to N_{qp_tot} | 21 |
| 12.6 | $dR_s/d\sigma_1$, responsivity of surface resistance R_s to σ_1 | 22 |
| 12.7 | $dX_s/d\sigma_2$, responsivity of surface reactance X_s to σ_2 | 22 |
| 12.8 | $d\lambda_{bqp}/dR_s$, responsivity of quasiparticle loss factor λ_{bqp} to surface resistance R_s | 23 |

| | | |
|-----------|---|-----------|
| 12.9 | dx_dX_s , responsivity of frequency detuning x to surface reactance X_s | 23 |
| 12.10 | $dQ_{qp}dR_s$, responsivity of quasiparticle quality factor Q_{qp} to surface resistance R_s | 24 |
| 13 | S21 | 24 |
| 13.1 | S21, resonator quality factor of resonator circuit in thin film local limit . . . | 24 |
| 14 | NEP | 24 |
| 14.1 | nep_{phot} , noise equivalent power (NEP) of photon noise | 24 |
| 14.2 | nep_{rec} , noise equivalent power (NEP) of recombination noise due to P_{opt} . | 25 |
| 15 | Finding P_{opt} | 25 |
| 15.1 | $P_{opt,r}$, P_{opt} value from f_{new} | 25 |
| 16 | What doesn't work yet | 26 |
| 16.1 | f_0 resonance frequency | 26 |
| 16.2 | f_{frac} too low | 26 |
| 16.3 | Q_r too low or drops too quickly | 28 |

1 Empirical inputs

| Input | Value | Confidence |
|---|-----------------------------------|------------|
| wI, width of inductor | $4 \times 10^{-6} \text{ m}$ | 100% |
| lI, length of inductor | $4 \times 10^{-4} \text{ m}$ | 100% |
| tI, thickness of inductor | $1.8 \times 10^{-8} \text{ m}$ | 100% |
| Tc, critical temperature | 1.4 K | 100% |
| tau0, characteristic electron-phonon interaction time | $4.38 \times 10^{-7} \text{ s}$ | 0% |
| T, operating temperature | 0.1 K | 100% |
| R_nsp, normal sheet resistivity | 90 Ohms/square | 100% |
| lamb, wavelength of photons | $1.1 \times 10^{-3} \text{ m}$ | 100% |
| delta_nuopt, optical bandwidth | $1 \times 10^{10} \text{ Hz}$ | 90% |
| Lg, geometric inductance | $3 \times 10^{-9} \text{ H}$ | 100% |
| C, capacitor capacitance in circuit | $5 \times 10^{-12} \text{ F}$ | 100% |
| eta_opt, optical efficiency | 0.8 | 100% |
| eta_pb, pair-breaking efficiency | 0.57 | 100% |
| tau_phon_br, time for phonon to break Cooper pair | $1 \times 10^{-10} \text{ s}$ | 0% |
| Qc, coupling quality factor | 5×10^4 | 100% |
| nqp0, quasiparticle density at 0K | $1 \times 10^{20} \text{ m}^{-3}$ | 100% |
| P_read, readout power | $6.31 \times 10^{-12} \text{ W}$ | 0% |
| T_amp, amplifier noise temperature | 3 K | 0% |
| deltav_read, readout bandwidth | 50 Hz | 0% |
| V_read, readout voltage | $1.776 \times 10^{-5} \text{ V}$ | 0% |

Table 1: Empirical inputs

2 Constants

2.1 VI, volume of inductor

| Input | Confidence |
|---------------------------|------------|
| wI, width of inductor | 100% |
| lI, length of inductor | 100% |
| tI, thickness of inductor | 100% |

Table 2: Inputs to VI, volume of inductor

$$V_I = w_I l_I t_I$$

2.2 nsq, number of squares of inductor

| Input | Confidence |
|------------------------|------------|
| wI, width of inductor | 100% |
| lI, length of inductor | 100% |

Table 3: Inputs to nsq, number of squares of inductor

$$n_{\text{sq}} = \frac{w_I}{l_I}$$

2.3 nu_opt, frequency of photons

| Input | Confidence |
|-----------------------------|------------|
| lamb, wavelength of photons | 100% |

Table 4: Inputs to nu_opt, frequency of photons

$$\nu_{\text{opt}} = c\lambda$$

2.4 E_gamma, energy of photons

| Input | Confidence |
|------------------------------|------------|
| nu_opt, frequency of photons | 100% |

Table 5: Inputs to E_gamma, energy of photons

$$E_{\gamma} = h\nu_{\text{opt}}$$

2.5 delta0, gap energy at 0K

Flanigan p.20 and Jay

| Input | Confidence |
|--------------------------|------------|
| Tc, critical temperature | 100% |

Table 6: Inputs to delta0, gap energy at 0K

$$\Delta_0 = 1.764kT_c$$

2.6 delta, gap energy at T

Zmuidzinas eq.4, basically identical to delta0.

| Input | Confidence |
|--------------------------|------------|
| delta0, gap energy at 0K | 100% |

Table 7: Inputs to delta, gap energy at T

$$\Delta = \Delta_0 \left(1 - \sqrt{2\pi k \Delta_0} e^{\frac{\Delta_0}{kT}} \right)$$

2.7 sigma_n, normal conductivity just above Tc

Flanigan (private correspondence)

| Input | Confidence |
|---------------------------------|------------|
| R_nsp, normal sheet resistivity | 100% |
| tI, thickness of inductor | 100% |

Table 8: Inputs to sigma_n, normal conductivity just above Tc

$$\sigma_n = \frac{1}{R_{\text{nsq}} t_I}$$

2.8 lambL, (London) penetration depth in the thin film limit

Zmuidzinas eq.12 (currently unused)

| Input | Confidence |
|--|------------|
| sigma_n, normal conductivity just above Tc | 50% |
| tI, thickness of inductor | 100% |

Table 9: Inputs to lambL, (London) penetration depth in the thin film limit

$$\lambda_L = \frac{\hbar}{\pi \mu_0 t_I \Delta \sigma_n}$$

2.9 N0, single-spin density of electron states at Fermi energy

Flanigan eq.3.10

| Input | Confidence |
|--------------------------|------------|
| T, operating temperature | 100% |
| delta0, gap energy at 0K | 100% |

Table 10: Inputs to N0, single-spin density of electron states at Fermi energy

$$N_0 = \frac{n_{\text{qp},0}}{2\sqrt{2\pi kT}\Delta_0 e^{-\frac{\Delta_0}{kT}}}$$

2.10 N_qp_photon, number of quasiparticles produced per photon

Flanigan eq.3.67

| Input | Confidence |
|----------------------------------|------------|
| eta_pb, pair-breaking efficiency | 100% |
| nu_opt, frequency of photons | 100% |
| delta, gap energy at T | 100% |

Table 11: Inputs to N_qp_photon, number of quasiparticles produced per photon

$$N_{\text{qp,phot}} = \frac{h\eta_{\text{pb}}\nu_{\text{opt}}}{\Delta}$$

3 Intrinsic parameters (intrinsic to material)

3.1 R_qp, intrinsic quasiparticle recombination constant

Flanigan eq.3.14

| Input | Confidence |
|--|------------|
| delta0, gap energy at 0K | 100% |
| N0, single-spin density of electron states at Fermi energy | 90% |
| tau0, characteristic electron-phonon interaction time | 0% |

Table 12: Inputs to R_qp, intrinsic quasiparticle recombination constant

$$R_{\text{qp}} = \frac{2 \left(\frac{\Delta_0}{kT_c} \right)^3}{N_0 \Delta_0 \tau_0}$$

4 Thermal parameters (depend on T)

4.1 n_qp_therm, quasiparticle density due to thermal effects at T

Flanigan eq.3.10

| Input | Confidence |
|--|------------|
| delta0, gap energy at 0K | 100% |
| N0, single-spin density of electron states at Fermi energy | 90% |
| T, operating temperature | 100% |

Table 13: Inputs to n_qp_therm, quasiparticle density due to thermal effects at T

$$n_{\text{qp,therm}} = 2N_0 \sqrt{2\pi kT \Delta_0} e^{-\frac{\Delta_0}{kT}}$$

4.2 gamma_G, low-temperature thermal generation rate at T

Flanigan eq.3.17

| Input | Confidence |
|--|------------|
| delta0, gap energy at 0K | 100% |
| N0, single-spin density of electron states at Fermi energy | 90% |
| tau0, characteristic electron-phonon interaction time | 0% |
| T, operating temperature | 100% |
| Tc, critical temperature | 100% |

Table 14: Inputs to gamma_G, low-temperature thermal generation rate at T

$$\gamma_G = \frac{16N_0 \Delta_0^3 \pi T}{\tau_0 k^2 T_c^3} e^{-\frac{2\Delta_0}{kT}}$$

5 Steady-state parameters

5.1 tau_phon_es, phonon escape time

Flanigan eq.3.19 (currently unused)

| Input | Confidence |
|--|------------|
| tI, thickness of inductor | 100% |
| eta_phon_trans, transmission probability per encounter | 0% |
| s, probably speed of sound | 0% |

Table 15: Inputs to tau_phon_es, phonon escape time

$$\tau_{\text{phon,es}} = \frac{4t_I}{s\eta_{\text{phon,es}}}$$

$$\eta_{\text{phon,es}} = 1 \times 10^{-9}$$

$$s = 6.4 \times 10^3 \text{ ms}^{-1}$$

5.2 F_phon, phonon trapping factor

Flanigan eq.3.20 (currently unused)

| Input | Confidence |
|---|------------|
| tau_phon_br, time for phonon to break Cooper pair | 0% |
| tau_phon_es, phonon escape time | 0% |

Table 16: Inputs to F_phon, phonon trapping factor

$$F_{\text{phon}} = 1 + \frac{\tau_{\text{phon,es}}}{\tau_{\text{phon,br}}}$$

5.3 R_eff, effective quasiparticle recombination constant

Flanigan p.31 (currently ignores F_phon)

| Input | Confidence |
|--|------------|
| R_qp, intrinsic quasiparticle recombination constant | 0% |
| F_phon, phonon trapping factor | 0% |

Table 17: Inputs to R_eff, effective quasiparticle recombination constant

$$R_{\text{eff}} = \frac{R_{\text{qp}}}{F_{\text{phon}}}$$

5.4 tau_qp, quasiparticle relaxation time

Flanigan p.46 (currently unused)

| Input | Confidence |
|---|------------|
| R_eff, effective quasiparticle recombination constant | 0% |
| gamma_G, low-temperature thermal generation rate at T | 0% |

Table 18: Inputs to tau_qp, quasiparticle relaxation time

$$\tau_{qp} = \frac{1}{\sqrt{4R_{\text{eff}}\gamma_G}}$$

5.5 n_qp_ss, steady-state quasiparticle density

Flanigan p.43. Should match nqp0, assuming ignoring F_phon. tau0 term cancels out from R_eff and gamma_G.

| Input | Confidence |
|---|------------|
| R_eff, effective quasiparticle recombination constant | 0% |
| gamma_G, low-temperature thermal generation rate at T | 0% |

Table 19: Inputs to n_qp_ss, steady-state quasiparticle density

$$n_{qp,ss} = \sqrt{\frac{\gamma_G}{R_{\text{eff}}}}$$

5.6 N_qp_ss, steady-state quasiparticle number in resonator

Flanigan p.57. tau0 term cancels out from R_eff and gamma_G.

| Input | Confidence |
|---|------------|
| R_eff, effective quasiparticle recombination constant | 0% |
| gamma_G, low-temperature thermal generation rate at T | 0% |
| VI, volume of inductor | 100% |

Table 20: Inputs to N_qp_ss, steady-state quasiparticle number in resonator

$$N_{qp,ss} = \sqrt{\frac{V_I\gamma_G}{R_{\text{eff}}}}$$

6 Optical generation

6.1 gamma_opt, constant optical power quasiparticle generation rate

Flanigan eq.3.68

| Input | Confidence |
|---|------------|
| P_opt, incident optical power | 100% |
| dGamma_dP, responsivity of quasiparticle generation rate to optical power | 100% |
| eta_pb, pair-breaking efficiency | 100% |
| delta, gap energy at T | 100% |

Table 21: Inputs to gamma_opt, constant optical power quasiparticle generation rate

$$\gamma_{\text{opt}} = \frac{dP_{\text{abs}}}{dP_{\text{inc}}} \frac{P_{\text{opt}} \eta_{\text{pb}}}{\Delta}$$

7 All together now

7.1 N_qp_tot, total number of quasiparticles in resonator due to thermal and constant optical power effects

Flanigan p.57. tau0 term cancels out between R_eff and gamma_G, but not between R_eff and gamma_opt. Effects are transmitted forward to fnew and Q_qp.

| Input | Confidence |
|---|------------|
| P_opt, incident optical power | 100% |
| gamma_opt, constant optical power quasiparticle generation rate | 100% |
| R_eff, effective quasiparticle recombination constant | 0% |
| gamma_G, low-temperature thermal generation rate at T | 0% |
| VI, volume of inductor | 100% |

Table 22: Inputs to N_qp_tot, total number of quasiparticles in resonator due to thermal and constant optical power effects

$$N_{\text{qp,tot}} = \sqrt{\frac{VI(\gamma_G + \gamma_{\text{opt}}(P_{\text{opt}}))}{R_{\text{eff}}}}$$

8 Complex conductivity

8.1 sigma1_0, real part of complex conductivity at T=0K

Flanigan p.35

| Input | Confidence |
|-------|------------|
|-------|------------|

Table 23: Inputs to sigma1_0, real part of complex conductivity at T=0K

$$\sigma_1(0) = 0$$

8.2 sigma2_0, imag part of complex conductivity at T=0K

Flanigan p.35

| Input | Confidence |
|--|------------|
| sigma_n, normal conductivity just above Tc | 100% |
| delta0, gap energy at 0K | 100% |
| f, readout frequency | 100% |

Table 24: Inputs to sigma2_0, imag part of complex conductivity at T=0K

$$\sigma_2(0) = \frac{\pi \Delta_0 \sigma_n}{hf}$$

8.3 signalrat, ratio of real part of complex conductivity to quasiparticle density response at T

Flanigan eq.3.79. Used in dsig1_dN.

| Input | Confidence |
|------------------------------|------------|
| delta0, gap energy at 0K | 100% |
| nu_opt, frequency of photons | 100% |
| T, operating temperature | 100% |

Table 25: Inputs to signalrat, ratio of real part of complex conductivity to quasiparticle density response at T

$$\Upsilon_{\sigma_1} = \sqrt{\frac{8\Delta_0}{\pi^3 kT}} \sinh \frac{h\nu_{\text{opt}}}{2kT} K_0 \left(\frac{h\nu_{\text{opt}}}{2kT} \right)$$

8.4 sigma2rat, ratio of imag part of complex conductivity to quasiparticle density response at T

Flanigan eq.3.80. Used in dsig2_dN.

| Input | Confidence |
|------------------------------|------------|
| delta0, gap energy at 0K | 100% |
| nu_opt, frequency of photons | 100% |
| T, operating temperature | 100% |

Table 26: Inputs to sigma2rat, ratio of imag part of complex conductivity to quasiparticle density response at T

$$\Upsilon_{\sigma_2} = -1 - \sqrt{\frac{2\Delta_0}{\pi kT}} e^{-\frac{h\nu_{\text{opt}}}{2kT}} I_0\left(\frac{h\nu_{\text{opt}}}{2kT}\right)$$

8.5 sigma1, real part of complex conductivity at T

Uses dsig1_dN.

| Input | Confidence |
|---|------------|
| P_opt, incident optical power | 100% |
| N_qp_tot, total number of quasiparticles in resonator | 90% |
| sigma1_0, real part of complex conductivity at T=0K | 100% |
| dsig1_dN, responsivity of sigma1 against N_qp_tot | 100% |
| f, readout frequency | 100% |

Table 27: Inputs to sigma1, real part of complex conductivity at T

$$\sigma_1(f) = N_{\text{qp,tot}}(P_{\text{opt}}) \frac{d\sigma_1(f)}{dN_{\text{qp}}} + \sigma_1(0)$$

8.6 sigma2, imag part of complex conductivity at T

Uses dsig2_dN.

| Input | Confidence |
|---|------------|
| P_opt, incident optical power | 100% |
| N_qp_tot, total number of quasiparticles in resonator | 90% |
| sigma2_0, imag part of complex conductivity at T=0K | 100% |
| dsig2_dN, responsivity of sigma2 against N_qp_tot | 100% |
| f, readout frequency | 100% |

Table 28: Inputs to sigma2, imag part of complex conductivity at T

$$\sigma_2(f) = N_{\text{qp,tot}}(P_{\text{opt}}) \frac{d\sigma_2(f)}{dN_{\text{qp}}} + \sigma_2(f, 0)$$

8.7 sigma, complex conductivity at T

Flanigan p.34

| Input | Confidence |
|--|------------|
| P_opt, incident optical power | 100% |
| sigma1, real part of complex conductivity at T | 90% |
| sigma2, imag part of complex conductivity at T | 90% |
| f, readout frequency | 100% |

Table 29: Inputs to sigma, complex conductivity at T

$$\sigma(f) = \sigma_1(f, P_{\text{opt}}) - i\sigma_2(f, P_{\text{opt}})$$

9 Surface impedance, reactance, (kinetic) inductance, resistance

9.1 Zs_0, surface impedance in thin film local limit at T=0K

Flanigan eq.3.35

| Input | Confidence |
|---|------------|
| sigma2_0, imag part of complex conductivity at T=0K | 100% |
| tI, thickness of inductor | 100% |
| f, readout frequency | 100% |

Table 30: Inputs to Zs_0, surface impedance in thin film local limit at T=0K

$$Z_s(f, 0) = \frac{i}{t_I \sigma_2(f, 0)}$$

9.2 Zs, surface impedance in thin film local limit at T

Flanigan eq.3.35

| Input | Confidence |
|----------------------------------|------------|
| P_opt, incident optical power | 100% |
| sigma, complex conductivity at T | 90% |
| tI, thickness of inductor | 100% |
| f, readout frequency | 100% |

Table 31: Inputs to Zs, surface impedance in thin film local limit at T

$$Z_s(f) = \frac{1}{t_I \sigma(f, P_{\text{opt}})}$$

9.3 Xs_0, surface reactance in thin film local limit at T=0K

Flanigan p.36

| Input | Confidence |
|--|------------|
| Zs_0, surface impedance in thin film local limit at T=0K | 100% |
| f, readout frequency | 100% |

Table 32: Inputs to Xs_0, surface reactance in thin film local limit at T=0K

$$X_s(f, 0) = \Im(Z_s(f, 0))$$

9.4 Xs, surface reactance in thin film local limit at T

Flanigan p.36

| Input | Confidence |
|---|------------|
| P_opt, incident optical power | 100% |
| Zs, surface impedance in thin film local limit at T | 90% |
| f, readout frequency | 100% |

Table 33: Inputs to Xs, surface reactance in thin film local limit at T

$$X_s(f) = \Im(Z_s(f, P_{\text{opt}}))$$

9.5 Rs, surface resistance in thin film local limit at T

Flanigan p.36

| Input | Confidence |
|---|------------|
| P_opt, incident optical power | 100% |
| Zs, surface impedance in thin film local limit at T | 90% |
| f, readout frequency | 100% |

Table 34: Inputs to Rs, surface resistance in thin film local limit at T

$$R_s(f) = \Re(Z_s(f, P_{\text{opt}}))$$

9.6 Lk_0, kinetic inductance in thin film local limit at T=0K

Flanigan p.36

| Input | Confidence |
|--|------------|
| nsq, number of squares of inductor | 100% |
| tI, thickness of inductor | 100% |
| delta0, gap energy at 0K | 100% |
| sigma_n, normal conductivity just above Tc | 100% |

Table 35: Inputs to Lk_0, kinetic inductance in thin film local limit at T=0K

$$L_k(0) = \frac{n_{\text{sq}} h}{2\pi^2 t_I \Delta_0 \sigma_n}$$

9.7 Lk, kinetic inductance in thin film local limit at T

Flanigan p.36

| Input | Confidence |
|--|------------|
| P_opt, incident optical power | 100% |
| tI, thickness of inductor | 100% |
| delta0, gap energy at 0K | 100% |
| sigma_n, normal conductivity just above Tc | 100% |
| N0, single-spin density of electron states at Fermi energy | 90% |
| VI, volume of inductor | 100% |

Table 36: Inputs to Lk, kinetic inductance in thin film local limit at T

$$L_k = L_k(0) \left(1 - \frac{N_{\text{qp,tot}}(P_{\text{opt}}) \Upsilon_{\sigma_2}}{2N_0 \Delta_0 V_I + N_{\text{qp,tot}}(P_{\text{opt}}) \Upsilon_{\sigma_2}} \right)$$

10 Resonant frequency

10.1 alpha, effective kinetic inductance fraction in thin film local limit

Flanigan eq.3.62

| Input | Confidence |
|---|------------|
| Lk_0, kinetic inductance in thin film local limit at T=0K | 100% |
| Lg, geometric inductance | 100% |

Table 37: Inputs to alpha, effective kinetic inductance fraction in thin film local limit

$$\alpha = \frac{L_k(0)}{L_g + L_k(0)}$$

10.2 f0, resonant frequency of resonator circuit at T=0K

Flanigan p.52

| Input | Confidence |
|---|------------|
| Lk_0, kinetic inductance in thin film local limit at T=0K | 100% |
| Lg, geometric inductance | 100% |
| C, capacitor capacitance in circuit | 100% |

Table 38: Inputs to f0, resonant frequency of resonator circuit at T=0K

$$f_0 = \frac{1}{2\pi\sqrt{C(L_g + L_k(0))}}$$

10.3 ffrac, fractional frequency shift in resonant frequency of circuit

Flanigan eq.3.63

| Input | Confidence |
|---|------------|
| alpha, effective kinetic inductance fraction in thin film local limit | 100% |
| P_opt, incident optical power | 100% |
| Lk, kinetic inductance in thin film local limit at T | 90% |
| Lk_0, kinetic inductance in thin film local limit at T=0K | 100% |

Table 39: Inputs to ffrac, fractional frequency shift in resonant frequency of circuit

$$s = \frac{\alpha}{2} \frac{L_k(P_{\text{opt}}) - L_k(0)}{L_k(0)}$$

10.4 fnew, resonant frequency of resonator circuit in thin film local limit

Flanigan eq.3.61

| Input | Confidence |
|--|------------|
| P_opt, incident optical power | 100% |
| f0, resonant frequency of resonator circuit at T=0K | 100% |
| ffrac, fractional frequency shift in resonant frequency of circuit | 90% |

Table 40: Inputs to fnew, resonant frequency of resonator circuit in thin film local limit

$$f_{\text{new}} = f_0(1 - s)$$

10.5 fdet, detuning of resonant frequency from readout frequency

Flanigan p.50

| Input | Confidence |
|--|------------|
| P_opt, incident optical power | 100% |
| f, readout frequency | 100% |
| fnew, resonant frequency of resonator circuit in thin film local limit | 90% |

Table 41: Inputs to fdet, detuning of resonant frequency from readout frequency

$$x = \frac{f}{f_{\text{new}}} - 1$$

11 Quality factors

11.1 Q_qp, quality factor of resonator circuit from quasiparticles

Flanigan eq.3.64

| Input | Confidence |
|---|------------|
| alpha, effective kinetic inductance fraction in thin film local limit | 100% |
| P_opt, incident optical power | 100% |
| Xs.0, surface reactance in thin film local limit at T=0K | 100% |
| Rs, surface resistance in thin film local limit at T | 90% |
| f, readout frequency | 100% |

Table 42: Inputs to Q_qp, quality factor of resonator circuit from quasiparticles

$$Q_{\text{qp}}(f) = \frac{X_s(f, 0)}{\alpha R_s(f, P_{\text{opt}})}$$

11.2 Qr, quality factor of resonator circuit in thin film local limit

Flanigan eq.3.58. Assumes internal quality factor Q_i is dominated by Q_qp.

| Input | Confidence |
|---|------------|
| P_opt, incident optical power | 100% |
| Q_qp, quality factor of resonator circuit from quasiparticles | 90% |
| Qc, coupling quality factor | 100% |
| f, readout frequency | 100% |

Table 43: Inputs to Qr, quality factor of resonator circuit in thin film local limit

$$Q_r = \left(\frac{1}{Q_c} + \frac{1}{Q_{qp}(f, P_{opt})} \right)^{-1}$$

12 Responsivities

12.1 dPabs_dPinc, responsivity of absorbed optical power to incident optical power

Flanigan eq.3.66

| Input | Confidence |
|-----------------------------|------------|
| eta_opt, optical efficiency | 100% |

Table 44: Inputs to dPabs_dPinc, responsivity of absorbed optical power to incident optical power

$$\frac{dP_{abs}}{dP_{inc}} = \eta_{opt}$$

12.2 dGamma_dP, responsivity of quasiparticle generation rate to optical power

Flanigan eq.3.69

| Input | Confidence |
|----------------------------------|------------|
| eta_pb, pair-breaking efficiency | 100% |
| delta0, gap energy at 0K | 100% |

Table 45: Inputs to dGamma_dP, responsivity of quasiparticle generation rate to optical power

$$\frac{d\gamma_{opt}}{dP_{opt}} = \frac{\eta_{pb}}{\Delta_0}$$

12.3 dN_qp_tot_dGamma, responsivity of N_qp_tot to quasiparticle generation rate

Flanigan eq.3.72

| Input | Confidence |
|---|------------|
| P_opt, incident optical power | 100% |
| gamma_opt, constant optical power quasiparticle generation rate | 100% |
| R_eff, effective quasiparticle recombination constant | 0% |
| gamma_G, low-temperature thermal generation rate at T | 0% |
| VI, volume of inductor | 100% |

Table 46: Inputs to dN_qp_tot.dGamma, responsivity of N_qp_tot to quasiparticle generation rate

$$\frac{dN_{\text{qp,tot}}}{d\gamma} = \frac{1}{2} \sqrt{\frac{V_I}{R_{\text{eff}}(\gamma_G + \gamma_{\text{opt}}(P_{\text{opt}}))}}$$

12.4 dsig1_dN, responsivity of sigma1 to N_qp_tot

Flanigan eq.3.81. Uses sigma1rat and used in calculation of sigma1.

| Input | Confidence |
|--|------------|
| sigma2_0, imag part of complex conductivity at T=0K | 100% |
| sigma1rat, ratio of real part of complex conductivity to quasiparticle density response at T | 100% |
| N0, single-spin density of electron states at Fermi energy | 100% |
| delta0, gap energy at 0K | 100% |
| VI, volume of inductor | 100% |
| f, readout frequency | 100% |

Table 47: Inputs to dsig1_dN, responsivity of sigma1 to N_qp_tot

$$\frac{d\sigma_1(f)}{dN_{\text{qp,tot}}} = \frac{\sigma_2(f, 0)\Upsilon_{\sigma_1}}{2N_0\Delta_0V_I}$$

12.5 dsig2_dN, responsivity of sigma2 to N_qp_tot

Flanigan eq.3.82. Uses sigma2rat and used in calculation of sigma2.

| Input | Confidence |
|--|------------|
| sigma2_0, imag part of complex conductivity at T=0K | 100% |
| sigma2rat, ratio of real part of complex conductivity to quasiparticle density response at T | 100% |
| N0, single-spin density of electron states at Fermi energy | 100% |
| delta0, gap energy at 0K | 100% |
| VI, volume of inductor | 100% |
| f, readout frequency | 100% |

Table 48: Inputs to dsig2_dN, responsivity of sigma2 to N_qp_tot

$$\frac{d\sigma_2(f)}{dN_{qp,tot}} = \frac{\sigma_2(f, 0)\Upsilon_{\sigma_2}}{2N_0\Delta_0 V_I}$$

12.6 dRs_dsig1, responsivity of surface resistance Rs to sigma1

Flanigan eq.3.83

| Input | Confidence |
|--|------------|
| Xs_0, surface reactance in thin film local limit at T=0K | 100% |
| sigma2_0, imag part of complex conductivity at T=0K | 100% |
| f, readout frequency | 100% |

Table 49: Inputs to dRs_dsig1, responsivity of surface resistance Rs to sigma1

$$\frac{dR_s(f)}{d\sigma_1} = \frac{X_s(f, 0)}{\sigma_2(f, 0)}$$

12.7 dXs_dsig2, responsivity of surface reactance Xs to sigma2

Flanigan eq.3.84

| Input | Confidence |
|--|------------|
| Xs_0, surface reactance in thin film local limit at T=0K | 100% |
| sigma2_0, imag part of complex conductivity at T=0K | 100% |
| f, readout frequency | 100% |

Table 50: Inputs to dXs_dsig2, responsivity of surface reactance Xs to sigma2

$$\frac{dX_s(f)}{d\sigma_2} = -\frac{X_s(f, 0)}{\sigma_2(f, 0)}$$

12.8 dlambqp_dRs, responsivity of quasiparticle loss factor lambda_qp to surface resistance Rs

Flanigan eq.3.87

| Input | Confidence |
|---|------------|
| alpha, effective kinetic inductance fraction in thin film local limit | 100% |
| P_opt, incident optical power | 100% |
| Xs_0, surface reactance in thin film local limit at T=0K | 100% |
| f, readout frequency | 100% |

Table 51: Inputs to dlambqp_dRs, responsivity of quasiparticle loss factor lambda_qp to surface resistance Rs

$$\frac{d\lambda_{qp}}{dR_s(f)} = \frac{\alpha(P_{opt})}{X_s(f, 0)}$$

12.9 dx_dXs, responsivity of frequency detuning x to surface reactance Xs

Flanigan eq.3.88

| Input | Confidence |
|---|------------|
| alpha, effective kinetic inductance fraction in thin film local limit | 100% |
| P_opt, incident optical power | 100% |
| Xs_0, surface reactance in thin film local limit at T=0K | 100% |
| f, readout frequency | 100% |

Table 52: Inputs to dx_dXs, responsivity of frequency detuning x to surface reactance Xs

$$\frac{dx}{dX_s(f)} = \frac{\alpha(P_{opt})}{2X_s(f, 0)}$$

12.10 dQqp_dRs, responsivity of quasiparticle quality factor Q_qp to surface resistance Rs

| Input | Confidence |
|---|------------|
| alpha, effective kinetic inductance fraction in thin film local limit | 100% |
| P_opt, incident optical power | 100% |
| Q_qp, quality factor of resonator circuit from quasiparticles | 100% |
| Xs_0, surface reactance in thin film local limit at T=0K | 100% |
| f, readout frequency | 100% |

Table 53: Inputs to dQqp_dRs, responsivity of quasiparticle quality factor Q_qp to surface resistance Rs

$$\frac{dQ_{qp}(f)}{dR_s(f)} = -\frac{Q_{qp}(f)^2 \alpha(P_{opt})}{X_s(f, 0)}$$

13 S21

13.1 S21, resonator quality factor of resonator circuit in thin film local limit

Flanigan eq.3.60

| Input | Confidence |
|---|------------|
| P_opt, incident optical power | 100% |
| f, readout frequency | 100% |
| Q_r, quality factor of resonator circuit in thin film local limit | 90% |
| Qc, coupling quality factor | 100% |
| fdet, detuning of resonant frequency from readout frequency | 90% |
| A, symmetry factor | 90% |

Table 54: Inputs to S21, resonator quality factor of resonator circuit in thin film local limit

$$S_{21} = 1 - \frac{Q_r(f, P_{opt})(1 + iA)}{Q_c(1 + 2iQ_r(f, P_{opt})x(f, P_{opt}))}$$

14 NEP

14.1 nep_phot, noise equivalent power (NEP) of photon noise

Flanigan eq.5.5, from shot noise and wave noise

| Input | Confidence |
|--------------------------------|------------|
| P_opt, incident optical power | 100% |
| nu_opt, frequency of photons | 100% |
| delta_nuopt, optical bandwidth | 90% |

Table 55: Inputs to nep_phot, noise equivalent power (NEP) of photon noise

$$\text{NEP}(P_{\text{opt}}) = \sqrt{2 \left(h\nu P_{\text{opt}} + \frac{P_{\text{opt}}^2}{\Delta\nu} \right)}$$

14.2 nep_rec, noise equivalent power (NEP) of recombination noise due to P_opt

Flanigan eq.5.19

| Input | Confidence |
|----------------------------------|------------|
| P_opt, incident optical power | 100% |
| delta0, gap energy at 0K | 100% |
| eta_opt, optical efficiency | 100% |
| eta_pb, pair-breaking efficiency | 100% |

Table 56: Inputs to nep_rec, noise equivalent power (NEP) of recombination noise due to P_opt

$$\text{NEP}(P_{\text{opt}}) = 2\sqrt{\frac{\Delta_0 P_{\text{opt}}}{\eta_{\text{opt}}\eta_{\text{pb}}}}$$

15 Finding P_opt

15.1 P_opt_r, P_opt value from fnew

| Input | Confidence |
|---|------------|
| fnew, resonant frequency of resonator circuit | 100% |

Table 57: Inputs to P_opt_r, P_opt value from fnew

$$\begin{aligned}
L_k(P_{\text{opt}}) &= 2(L_g + L_k(T = 0))(1 - 2\pi f_{\text{new}} \sqrt{C(L_g + L_k(T = 0))}) + L_g \\
N_{\text{qp,tot}} &= -\frac{2N_0\Delta_0 V_I}{\Upsilon_{\sigma_2}} \left(1 + \frac{L_k(T = 0)}{L_k(P_{\text{opt}})} \right) \\
P_{\text{opt}} &= \frac{\Delta}{\eta_{\text{pb}}\eta_{\text{opt}}} \left(\frac{N_{\text{qp,tot}}^2 R_{\text{eff}}}{V_I} - \gamma_G \right)
\end{aligned}$$

16 What doesn't work yet

16.1 f0 resonance frequency

With parameters meant to have $f_{\text{new}}(0)=500$ MHz, i.e. $n_{\text{qp}0}=10^{20}$ and $R_{\text{nsq}}=90\ \Omega$, and τ_0 set at value for Al (4.38×10^{-7} s), actual $f_{\text{new}}(0)=1.281$ GHz. Linked to R_{nsq} .

16.2 ffrac too low

Fig. 1: With parameters set to have $f_{\text{new}}(0)=500$ kHz, i.e. $n_{\text{qp}0}=10^{20}$ and $R_{\text{nsq}}=1.7536 \times 10^4\ \Omega$, and τ_0 set at value for Al (4.38×10^{-7} s), f_{frac} changes very little with P_{opt} . Linked to $n_{\text{qp}0}$.

Fig. 2 and Fig. 3: With only change from default being $\tau_0=10$ s, f_{frac} follows empirical trend.

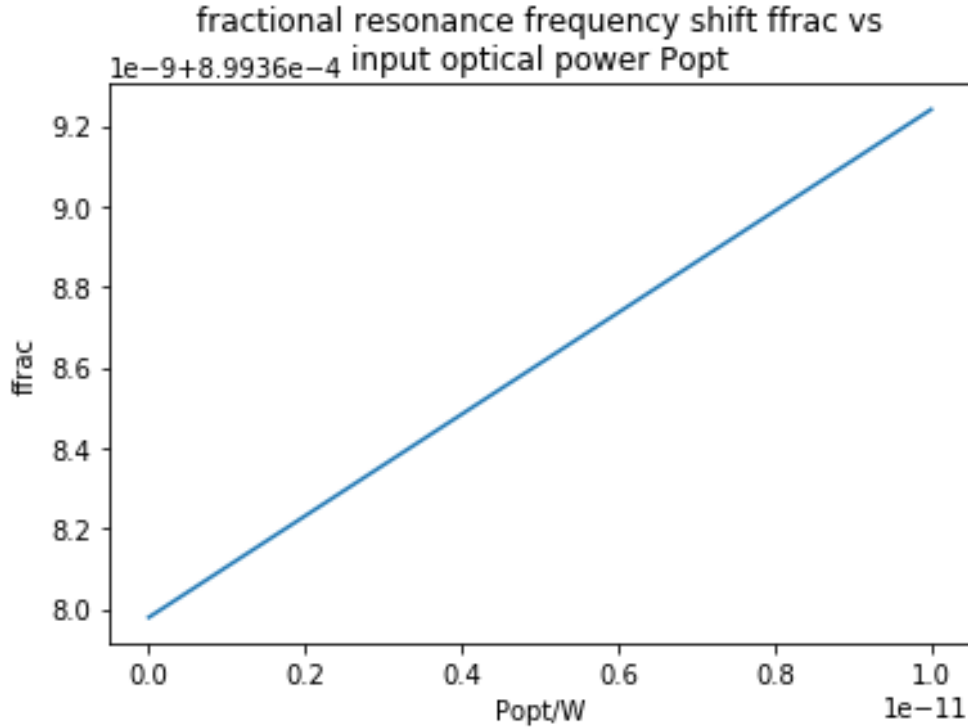


Figure 1: Fractional frequency shift with $R_{\text{nsq}}=1.7536 \times 10^4\ \Omega$ so $f_{\text{new}}(0)=500$ kHz.

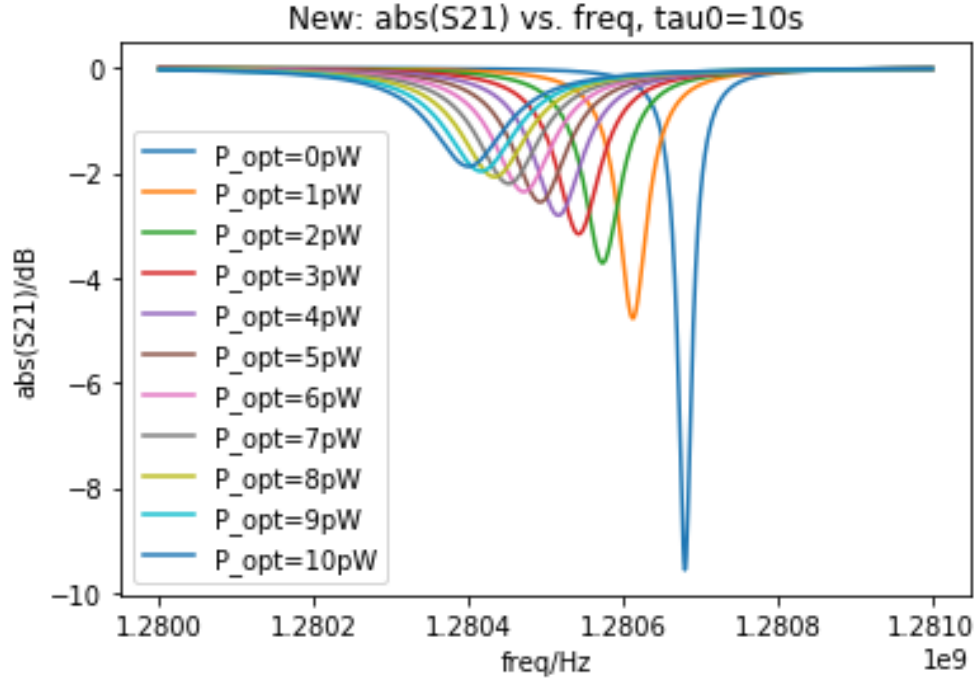


Figure 2: Resonance curves with only τ_0 changed from 4.38×10^{-7} s to 10 s.

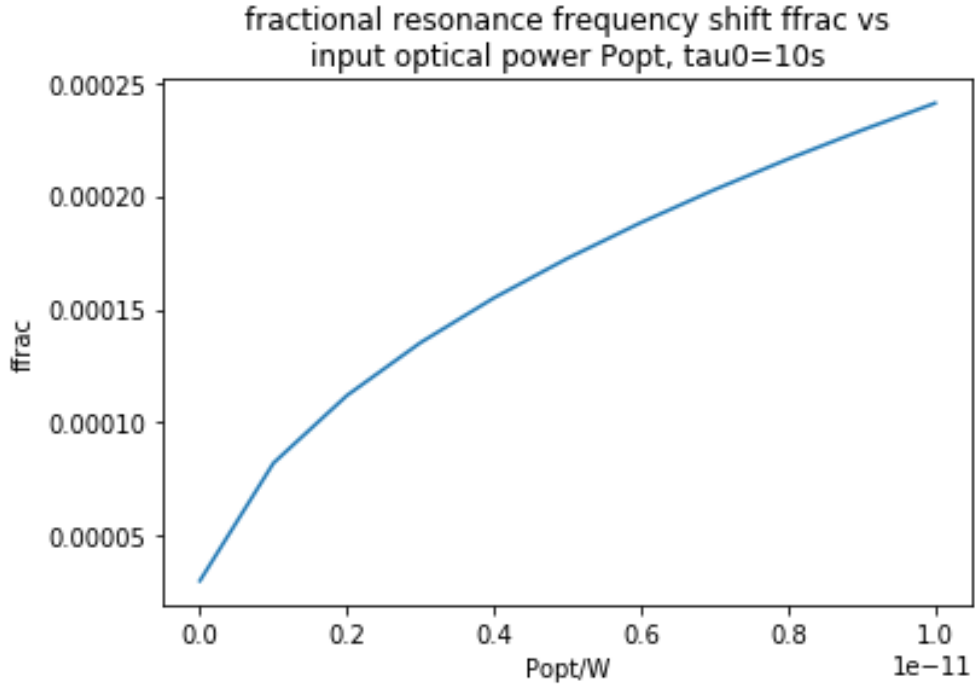


Figure 3: Fractional frequency shift with only τ_0 changed from 4.38×10^{-7} s to 10 s.

16.3 Qr too low or drops too quickly

Fig. 4: With parameters set to have $f_{\text{new}}(0)=500$ kHz and τ_0 set at value for Al (4.38×10^{-7} s), Q_r too low or drops too quickly with P_{opt} . Linked to n_{qp0} .

Fig. 5: With only change from default being $\tau_0=10$ s, Q_r follows empirical trend.

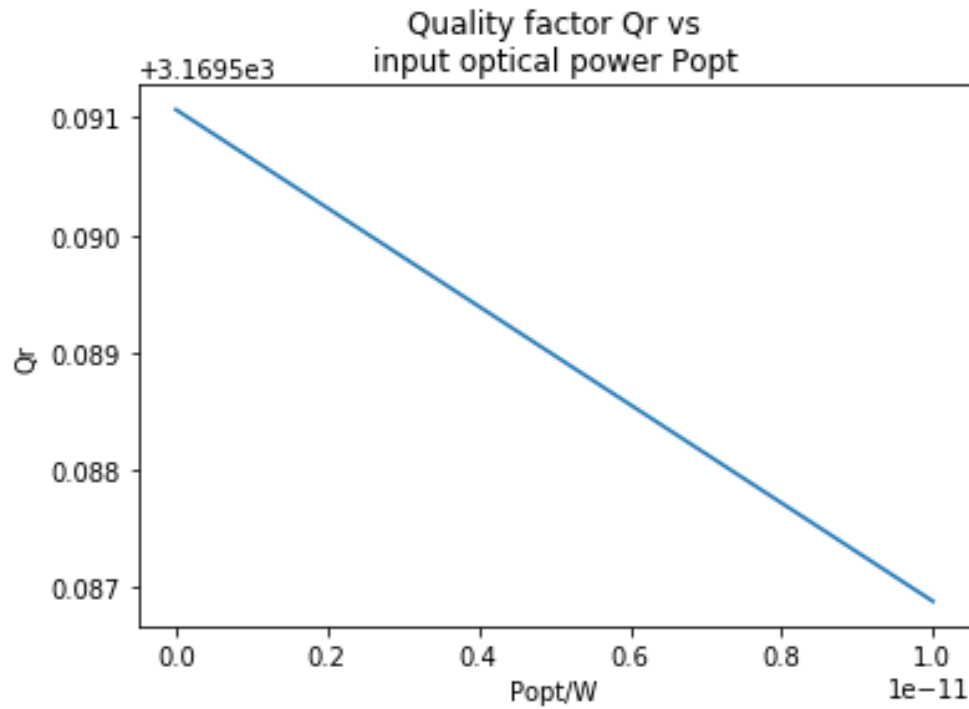


Figure 4: Quality factor with $R_{\text{nsq}}=1.7536 \times 10^4 \Omega$ so $f_{\text{new}}(0)=500$ kHz.

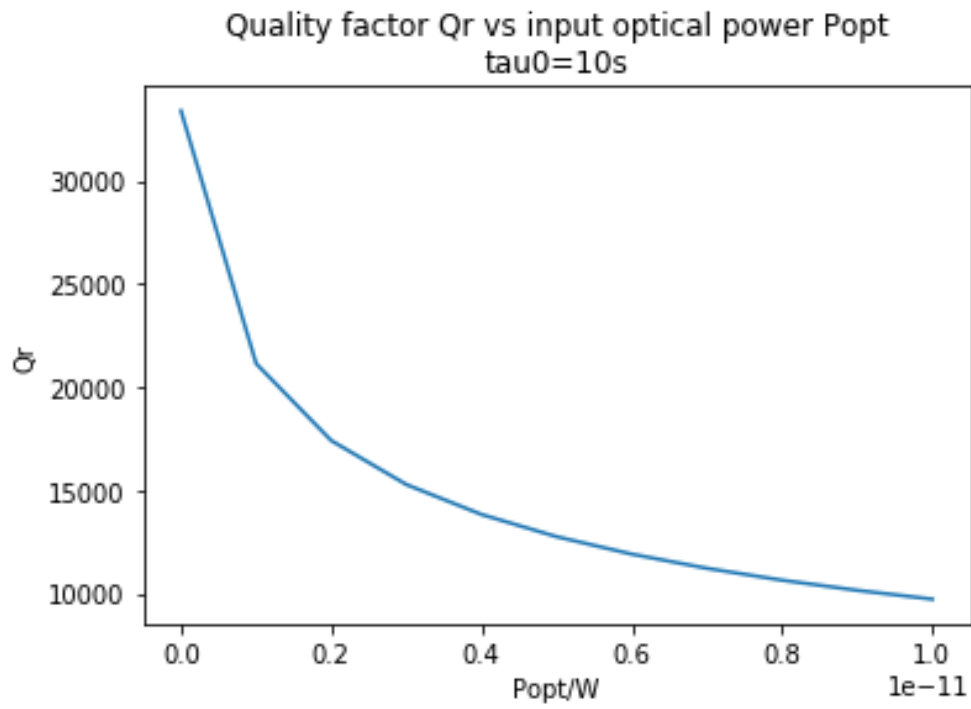


Figure 5: Quality factor with only τ_0 changed from $4.38 \times 10^{-7}\text{s}$ to 10s .